Lithosphere thickness controls the continental basalt compositions: An illustration using the Cenozoic basalts from eastern China

Pengyuan Guo [a, b, c, *], Yaoling Niu [a,b, d, e], Pu Sun [a, b, c], Hongmei Gong [a, b, c], Xiaohong Wang [a, b, c]

[a.] Institute of Oceanology, Chinese Academy of Sciences, Qingdao 266071, China

[b.] Qingdao National Laboratory for Marine Science and Technology, Qingdao 266061, China

[c.] Center for Ocean Mega-Science, Chinese Academy of Sciences, Qingdao 266071, China

[d.] Department of Earth Sciences, Durham University, Durham DH1 3LE, UK

[e.] School of Earth Science and Resources, China University of Geosciences, Beijing 100083, China

*Corresponding authors:

Dr. P.Y. Guo (guopy@qdio.ac.cn)

Current address:

Institute of Oceanology

Chinese Academy of Sciences

Nanhai Road 7

Qingdao, Shandong 266071

China

ABSTRACT

Recent studies demonstrate that the lithosphere thickness variation exerts the primary control on the global seafloor basalt compositions. If the mechanism of such control, i.e., the lid effect, is indeed at work, the lithosphere thickness variation must also influence the basaltic compositions in continental settings. To test this hypothesis, we choose to study the Cenozoic basalts in eastern continental China over a spatial distance of ~260 km along a NW-SE traverse with a steep topographic gradient (~1500 to ~500 m above sea level) corresponding to a steep lithospheric thickness gradient (~120 to ~90 km). The basalts erupted on the thickened lithosphere to the west are characterized by high pressure (e.g., low Si_{72}, high Mg_{72}, Fe_{72} and $[Sm/Yb]_N$) and lower extent (e.g., Ti_{72}, P_{72}, K_{72}, Rb, Ba, Th and higher more-to-less incompatible element ratios like $[La/Sm]_N$, Ba/Zr and Zr/Yb) of melting, whereas the basalts erupted on the thinned lithosphere to the east show the inverse. Importantly, these geochemical parameters all show significant correlations with both the lithosphere thickness and topographic elevation. These first order observations are straightforward manifestation of the lid effect. Lithospheric contamination and mantle source compositional variation can indeed contribute to the compositional variability of these continental basalts, but these latter effects are averaged out and are overshadowed by the lid effect. This finding emphasizes the importance of evaluating the lid effect before interpreting the petrogenesis of continental basalts and mantle dynamics. Our result also indicates that the continental surface elevation is isostatically balanced above a mantle depth that is deeper that the lithosphere-asthenosphere boundary.

INTRODUCTION

Basaltic magmas produced in continental settings have large compositional variations, petrologically from tholeiites to varying alkali-rich varieties (e.g., Dupuy & Dostal, 1984; Bell & Peterson, 1991; Guo et al., 2016). While factors such as source compositional variation (e.g., Lum et al., 1989), fractional crystallization (e.g., Peterson, 1989) and crustal contamination (Dupuy & Dostal, 1984; Ingle et al., 2004) can all affect the erupted basalt compositions, the lithosphere thickness effect on the compositional variation of the continental basalts has been largely overlooked despite the speculation in discussing the abundances and patterns of rare earth elements in oceanic basalts (e.g., Ellam, 1992) and implications in the experimental petrology (e.g., Green & Ringwood, 1967).

Recent studies on global seafloor basalts demonstrate that the lithosphere thickness variation exerts the primary control on the compositions of these basalts especially those erupted on intraplate ocean islands with varying lithosphere thickness at the time of eruption (Humphreys & Niu, 2009; Niu et al., 2011; Niu, 2016; Niu & Green, 2018). The basalts erupted on the thicker lithosphere have geochemical characteristics of lower extent (*F*) and higher pressure (*P*) of melting, whereas the basalts erupted on the thinner lithosphere have geochemical signatures of higher *F* and lower *P*. This is because $F \propto P_o – P_f$, where P_o is the initial depth of melting when the adiabatically upwelling asthenospheric mantle intersects the solidus and P_f is the depth of melting cessation and melt extraction when the decompression melting mantle encounters the lithosphere, which is the very depth of the lithosphere-asthenosphere boundary (LAB). This is the concept of the “lid effect” (see Niu et al., 2011), and its mechanism is simply to cap the decompression melting at the LAB (Niu & Green, 2018).

If this understanding is of general significance, then the "lid effect" must also be important in affecting basaltic magmatism in continental settings with the erupted basalts recording the lid effect as the result of varying lithosphere thickness.

To test the "lid effect" hypothesis for continental basalts and to evaluate the extent of this effect on the compositional variation of continental basalts, we choose to study the Cenozoic basalts in eastern continental China over a spatial distance of ~260 km in the Chifeng-Xilin Hot area along a NW-SE traverse with a steep topographic gradient (~1500 to ~500 m above sea level) corresponding to a steep lithospheric thickness gradient (~120 to ~90 km). The result is fully consistent with the lid effect. We note that source compositional variation and lithospheric contamination can contribute to the compositional variability of continental basalts, but these are secondary, and are averaged out with the mean compositions markedly reflecting the lid effect.

GEOLOGICAL BACKGROUND

The Cenozoic basaltic volcanism is widespread in eastern continental China, spatially from Wudalianchi in the northeast to the Hainan Island in the south (Fan & Hopper, 1991). Most of these volcanic rocks are alkali-rich varieties (e.g., Guo et al., 2016; Sun et al., 2017) with tholeiites also present in several locations (Zhi et al., 1998; Xu et al., 2005; Zou et al., 2000). Studies on these within-continent basalts reveal that these basalts are isotopically depleted relative to the bulk silicate earth with $\varepsilon_{Nd}(t) > 0$, $\varepsilon_{Hf}(t) > 0$, but highly enriched in incompatible elements and enriched in the progressively more incompatible elements (e.g., Guo et al., 2016, Sun et al., 2017), resembling the present-day ocean island basalts (OIBs). Based on the observation that the Pacific plate is subducting underneath the eastern Eurasian continent

(Huang & Zhao, 2009), and also the obvious lithosphere thickness contrasts between East and West continental China (Niu, 2005; Li et al., 2013), the western Pacific wedge suction induced eastward asthenosphere flow may be the ultimate cause of the asthenospheric mantle upwelling and decompression melting feeding for the Cenozoic basaltic volcanism in eastern China (e.g., Niu, 2005, 2014).

The Cenozoic basaltic volcanism in the Chifeng-Xilin Hot area is a type example of the Cenozoic volcanism in the region, with their eruption age ranging from ~23.8 Ma to ~0.19 Ma (Ho et al., 2008; Wang et al., 2015). These basalts spread over a spatial distance of ~260 km across the Great Gradient Line (GGL; Niu, 2005), a steep gradient in gravity, elevation, topography, crustal thickness, lithosphere thickness and heat flow between the high plateaus to the west and the hilly lowland plains in the east (Fig. 1A). As shown in Fig. 1B & C, Chifeng is to the east of the GGL and Xilin Hot is to the west of the GGL. Regionally, the high-resolution seismic tomography reveals significant changes in the depth of the lithosphere-asthenosphere boundary (LAB) beneath the Chifeng-Xilin Hot area, ranging from ~80 km beneath the Chifeng area to ~120 km beneath the Xilin Hot area (Fig. 1C). This LAB depth also correlates well with the surface elevation (Fig. 1C), reflecting the first-order isostatic equilibrium. The Chifeng-Xilin Hot Cenozoic basalts, thus, offer a prime opportunity to test the lid effect hypothesis in a continental setting.

SYSTEMATIC COMPOSITIONAL VARIATIONS OF THE CHIFENG-XILIN HOT BASALTS

We selected 19 new fresh samples from the three locations (solid symbols in Fig. 1B) for bulk-rock major element, trace element and Sr-Nd-Hf isotope compositional analysis. The analytical methods and results are given in the supplementary files. We also used the recently published data on 41 basaltic samples from the Chifeng-Xilin Hot area (half-filled symbols in Fig. 1B; Wang et al., 2015; Guo et al., 2016; Pang et al., 2019). In order to remove the effects of fractional crystallization, we corrected major element compositions of all these samples to $Mg^{\#}$ = 0.72, the minimum value to be in equilibrium with the mantle olivine, following Humphreys & Niu (2009) (see supplementary files).

Spatially, from southeast to northwest, these basalts change gradually from tholeiite (quartz normative) to transitional basalts (hypersthene normative) and to alkali basalts (nepheline normative) (Fig. S1). Fig. 2 plots major element compositions corrected to $Mg^{\#}$ = 0.72 as a function of distance relative to the most southeast sample (CF14-02) location calculated using the great circle distance (e.g., Niu & Batiza,1993), showing Si_{72} decreases, while Mg_{72}, Fe_{72}, Ti_{72}, P_{72}, K_{72} increase towards northwest. Such consistent spatial trends are also obvious for incompatible elements (Fig. S2), for ratios of highly-to-moderately incompatible elements (e.g., $[La/Sm]_N$, Rb/Hf, Ba/Zr) and for ratios of moderately-to-slightly incompatible elements (e.g., $[Sm/Yb]_N$, Hf/Lu, Zr/Yb) (Fig. 3). Despite the large incompatible element compositional variability (Fig. 2,3,S2), the Chifeng-Xilin Hot basalts generally display similarly depleted Sr-Nd-Hf isotope compositions relative to the bulk silicate earth, with $^{87}Sr/^{86}Sr$ = 0.70369-0.70443, $^{143}Nd/^{144}Nd$ = 0.512750-0.512931 and $^{176}Hf/^{177}Hf$ = 0.282926-0.283081 (Figs. S3 ,S4), implying their similar but still heterogeneous mantle source.

EVALUATION OF CRUSTAL MATERIAL CONTAMINATION

Continental crustal contamination during magma ascent is inevitable, but crustal contamination proxies, such as SiO_2/MgO, Ce/Pb, Nb/Th, Ta/U and $^{87}Sr/^{86}Sr$, $^{143}Nd/^{144}Nd$,

$^{176}Hf/^{177}Hf$ without coherent correlations, suggest that this effect is negligible (see Fig. S5). Furthermore, the occurrence of mantle xenoliths in Xilin Hot alkaline basalts (Fig. S6) indicates that they ascended rapidly, with limited interaction with the crust, which is supported by recent studies (Wang et al., 2015; Guo et al., 2016; Sun et al., 2018; Pang et al., 2019). Therefore, the observed major element and trace element compositional systematics in these basalts (Figs. 2, 3,4) largely reflect those of primary magmas parental to the basalts as the result of varying source composition or varying extent and pressure of mantle melting.

EVALUATION OF MANTLE SOURCE COMPOSITIONAL VARIATIONS

Generally, all these basalts have OIB-like incompatible element compositions with high $[La/Sm]_N$ (1.2-3.5) and $[Sm/Yb]_N$ (2.4-9.2), and are more enriched in the progressively more incompatible elements (Fig. S7), indicating (1) their derivation from varying low-degree melting of prior metasomatically enriched sources; and (2) the partial melting occurring in the sub-lithospheric mantle garnet stability field with garnet as a residual phase. These basalts also show OIB-like depleted Sr-Nd-Hf isotope compositions (Fig. S2) and elevated $[Nb/Th]_N$, $[Ta/U]_N$ (Fig. S8), which differ distinctively from those of the >110Ma alkali basalts in eastern China (Fig. S2 & S8), which are derived from melting of the continental lithospheric mantle. Therefore, these basalts originated from partial melting of metasomatized asthenospheric (vs. lithospheric) mantle. Furthermore, the lack of temporal and spatial variation of Sr-Nd-Hf isotopes of these basalts (Fig. S4) indicate that these basalts share similarly heterogenous asthenospheric mantle source in the Cenozoic.

LITHOSPHERE THICKNESS EFFECT ON BASALT COMPOSITIONS

In the Chifeng-Xilin Hot area, the lithosphere gradually thickens northwestward as indicated by the dotted line labeled LAB (Fig. 1C). This is well mirrored by the increasing surface elevation as the result of isostatic equilibrium. That is, the surface elevation positively correlates with the LAB depth. If the lid effect hypothesis is valid and applies here, we should see systematic variation in the compositions of these basalts as a function of the lithosphere thickness and surface elevation. This is indeed the case.

Figure 2 shows that the Chifeng-Xilin Hot basalts display decreasing Si_{72}, but increasing Mg_{72}, Fe_{72} and $[Sm/Yb]_N$ with increasing lithosphere thickness towards northwest, which are consistent with increasing pressure (depth) of melt extraction, P_f (Fig. 1D). The latter corresponds to the thickened lithosphere and is physically the very LAB depth (Niu and Green, 2018). Also, towards northwest, the basalts show increasing $[La/Sm]_N$, Rb/Hf, Hf/Lu, Ba/Zr and Zr/Yb, Ti_{72}, P_{72}, K_{72} and other incompatible elements (Figs. 2 & 3 and Fig. S2), which are consistent with the decreasing extent of melting. This is also consistent with the northwestward thickening lithosphere with deepening LAB that caps decompression melting and makes melt extraction at greater depths (Fig. 1D). Figure 4 shows the significant correlations of basalt compositions with surface elevation, which further illustrates the lithosphere thickness control (see above). All these coherent and systematic changes in basalt compositions with lithosphere thickness variation as well as surface elevation variation demonstrate the working of the lid effect on basaltic magmatism in continental settings.

Note that lithosphere thickening due to conductive heat loss to the surface is natural (see Niu and Green, 2018). In that case, the lithosphere in the Chifeng-Xilin Hot area would thicken with time in the Cenozoic. If so, we should expect basalt compositional variation as a function of eruption age, but this is not observed (Fig. S4), which is in fact understood because

(1) there is no evidence that the geotherm beneath the region has changed significantly over the past ~ 20 Myrs (Huang & Xu, 2010); (2) if the geotherm had cooled with time, the lithosphere beneath the younger volcanism to the southeast (i.e., Chifeng) would be thickened and thicker than the lithosphere beneath the older volcanism at the time of eruption to the northwest (i.e., Xilin Hot), but the opposite is true (Fig. 1c); (3) even if the cooling induced thickening had happened in the region due to heat loss in the past ~ 22 Myrs, the lithosphere beneath Chifeng at the time of volcanism would have to be ~ 10 km or more thinner about ~ 22 Myrs ago. In brief, the large compositional variation of the basalts along the NW-to-SE traverse (Figs. 2-3) is clearly consistent with the NW-to-SE lithosphere thickness variation across the prominent GGL (Fig. 1c-d).

CONCLUSIONS

Studies show that global OIB vary significantly in their compositions, but the lithosphere thickness (i.e., the depth of the LAB) at the time of OIB eruption exerts the primary control on OIB compositions in terms of the extent and pressure of melting. This is the “lid effect”, i.e., the lithosphere lid caps the upwelling and decompression melting mantle, resulting in melts erupted on the thin lithosphere having geochemical signatures of high extent and low pressure of melting, whereas melts erupted on the thick lithosphere showing the inverse. If the lid effect is globally significant, it should also be true on land. To test this hypothesis, we studied the Cenozoic basalts in eastern continental China (The Chifeng-Xilin Hot basalts) over a spatial distance of ~260 km along a NW-SE traverse across the GGL with a steep topographic gradient (~1500 to ~500 m above sea level) mirrored with a lithospheric thickness gradient (~120 to ~90 km). Our results demonstrate that the lid effect responsible for global OIB compositional systematics also operates in continental settings. That is, the continental lithosphere thickness (i.e., the LAB depth) variation exerts the primary control on basaltic compositions in terms of the extent and pressure melting, critically important for understating upper mantle dynamics and continental geology. Our results also provide strong evidence for isostatic equilibrium in the crust-mantle system above a mantle depth deeper than the LAB.

ACKNOWLEDGMENTS

This work was supported by the National Natural Science Foundation of China (grants 41776067, 41630968 and 91014003) and the 111 Project (B18048). We thank Yonghua Li, Chuanxu Chen, Wanfeng Chen and Guangxu Zhang for the help with geological map, tomography map and seismic tomography drawing.

REFFERENCES

Amante, C., and Eakins, B., 2009. Etopo1 1 arc-minute global relief model: Procedures, data sources and analysis. NOAA Technical Memorandum NESDIS NGDC-24. National Geophysical Data Center, NOAA.

Bell, K., and Peterson, T., 1991. Nd and Sr isotope systematics of Shombole volcano, East Africa, and the links between nephelinites, phonolites, and carbonatites. Geology, v. 19, p. 582-585.

Dupuy, C., and Dostal, J., 1984. Trace element geochemistry of some continental tholeiites. Earth and Planetary Science Letters, v. 67, p. 61-69.

Ellam, R.M., 1992. Lithospheric thickness as a control on basalt geochemistry. Geology, v. 20,

p. 153–156.

Fan, Q., and Hooper, P.R., 1991. The Cenozoic basaltic rocks of eastern China: petrology and chemical composition. Journal of Petrology, v. 32, p. 765-810.

Guo, P.Y., Niu, Y.L., Sun, P., Ye, L., Liu, J.J., Zhang, Y., ... and Zhao, J.X., 2016. The origin of Cenozoic basalts from central Inner Mongolia, East China: the consequence of recent mantle metasomatism genetically associated with seismically observed paleo-Pacific slab in the mantle transition zone. Lithos, v. 240, p. 104-118.

Green, D.H., and Ringwood, A.E., 1967. The genesis of basaltic magmas. Contributions to Mineralogy and Petrology, v. 15, p. 103-190.

Ho, K.S., Liu, Y.A.N., Chen, J.C., and Yang, H.J., 2008. Elemental and Sr-Nd-Pb isotopic compositions of late Cenozoic Abaga basalts, Inner Mongolia: Implications for petrogenesis and mantle process. Geochemical Journal, v. 42, p. 339-357.

Huang, J., and Zhao, D., 2006. High-resolution mantle tomography of China and surrounding regions. Journal of Geophysical Research, v. 111, (B9).

Huang, X.L., and Xu, Y.G., 2010. Thermal state and structure of the lithosphere beneath eastern China: a synthesis on basalt-borne xenoliths. Journal of Earth Science, v. 21, p. 711-730.

Humphreys, E.R., and Niu, Y.L., 2009. On the composition of ocean island basalts (OIB): The effects of lithospheric thickness variation and mantle metasomatism. Lithos, v. 112, p. 118-136.

Ingle, S., Scoates, J.S., Weis, D., Brügmann, G., and Kent, R.W., 2004. Origin of Cretaceous continental tholeiites in southwestern Australia and eastern India: insights from Hf and Os isotopes. Chemical Geology, v. 209, p. 83-106.

Li, Y., Wu, Q., Pan, J., Zhang, F., and Yu, D., 2013. An upper-mantle s -wave velocity model for east asia from rayleigh wave tomography. Earth and Planetary Science Letters, v. 377-378, p. 367-377.

Lum, C.C., Leeman, W.P., Foland, K.A., Kargel, J.A., and Fitton, J.G., 1989. Isotopic variations in continental basaltic lavas as indicators of mantle heterogeneity: Examples from the western US Cordillera. Journal of Geophysical Research, v. 94(B6), p. 7871-7884.

Niu, Y.L., and Green, D.H., 2018. The petrological control on the lithosphere-asthenosphere boundary (LAB) beneath ocean basins. Earth-Science Reviews v. 185, p. 301-307.

Niu, Y.L., 2005. Generation and evolution of basaltic magmas: some basic concepts and a new view on the origin of Mesozoic–Cenozoic basaltic volcanism in eastern China. Geological Journal of China Universities, v. 11, p. 9-46.

Niu, Y.L., 2014. Geological understanding of plate tectonics: Basic concepts, illustrations, examples and new perspectives. Global Tectonics and Metallogeny, v. 10, p. 23-46.

Niu, Y.L., Wilson, M., Humphreys, E.R., and O'Hara, M.J., 2011. The origin of intra-plate ocean island basalts (OIB): the lid effect and its geodynamic implications. Journal of Petrology, v. 52, p. 1443-1468.

Niu, Y.L., 2016. The meaning of global ocean ridge basalt major element compositions. Journal of Petrology, v. 57, p. 2081-2103.

Niu, Y.L., and Batiza, R., 1993. Chemical variation trends at fast and slow spreading mid-ocean ridges. Journal of Geophysical Research Solid Earth, v. 98, p. 7887-7902.

Pang, C.J., Wang, X.C., Li, C.F., Wilde, S.A., and Tian, L., 2019. Pyroxenite-derived Cenozoic basaltic magmatism in central Inner Mongolia, eastern China: Potential contributions from the subduction of the Paleo-Pacific and Paleo-Asian oceanic slabs in the Mantle Transition Zone. Lithos, v. 332, p. 39-54.

Peterson, T.D., 1989. Peralkaline nephelinites. Contributions to Mineralogy and Petrology, v. 102, p. 336-346.

Sun, P., Niu, Y.L., Guo, P.Y., Ye, L., Liu, J.J., and Feng, Y.X., 2017. Elemental and Sr–Nd–Pb isotope geochemistry of the Cenozoic basalts in Southeast China: Insights into their mantle sources and melting processes. Lithos, v. 272, p. 16-30.

Wang, X.C., Wilde, S.A., Li, Q.L., and Yang, Y.N., 2015. Continental flood basalts derived from the hydrous mantle transition zone. Nature communications, v. 6, 7700.

Xu, Y.G., Ma, J.L., Frey, F.A., Feigenson, M.D., and Liu, J.F., 2005. Role of lithosphere–asthenosphere interaction in the genesis of Quaternary alkali and tholeiitic basalts from Datong, western North China Craton. Chemical Geology, v. 224, p. 247-271.

Zhi, X.C., Song, Y., Frey, F.A., Feng, J.L., and Zhai, M.Z., 1990. Geochemistry of Hannuoba basalts, eastern China: constraints on the origin of continental alkalic and tholeiitic basalt. Chemical Geology, v. 88, p. 1-33.

Zou, H.B., Zindler, A., Xu, X.S., and Qu, Q., 2000. Major, trace element, and Nd, Sr and Pb isotopic studies of Cenozoic basalts in SE China: mantle sources, regional variations, and tectonic significance. Chemical Geology, v. 171, p. 35– 47.

FIGURE CAPTION

Fig. 1 (A) Topographic map of East Asia (data from Amante & Eakins, 2009). The Great Gradient Line is indicated as purple dashed line, which contrasts the high elevation and thickened lithosphere to the west from the low elevation and thinned lithosphere to the east. The study area is indicated with the rectangle with the A-B traverse used in subsequent figures. (B) Distribution and sample locations of the Chifeng-Xilin Hot Cenozoic basalts. The solid blue triangles, solid green diamonds and solid red circles represent sample locations in this study, and the half-filled diamonds and half-filled circles represent transitional basalt locations in the literature (Wang et al., 2015; Guo et al., 2016; Pang et al., 2019). (C) Top: topographic profile along the A-B section indicated in (a); bottom: vertical section of the shear-wave velocity tomography along the A-B traverse (based on the data in Li et al., 2013). (D) Cartoon illustrating the lithosphere thickness control on the geochemistry of erupted basaltic magmas.

Fig. 2 Systematic variation of the major element compositions of the Chifeng-Xilin Hot Cenozoic basalts as a function of distance relative to sample location CF14-02 parallel to the A-B traverse (Fig. 1B). The relative distance is calculated following Niu & Batiza (1993). The subscript 72 refers to the corresponding oxides corrected for fractionation effect to $Mg^{\#}=72$ (Humphreys and Niu, 2009) so as to discuss mantle sources and processes. The three bands with different colors indicate the thick, medium and thin lithosphere at the time of basalt eruption. The symbols are as in Fig. 1B.

Fig. 3 Systematic variation of the more-to-less incompatible element ratios of the Chifeng-Xilin Hot Cenozoic basalts plotted as a function of distance to sample location CF14-02 as in Fig. 2.

Fig. 4 Systematic variation of the major elements and more-to-less incompatible element ratios of the Chifeng-Xilin Hot Cenozoic basalts with sample (surface) elevation.

Fig. 1

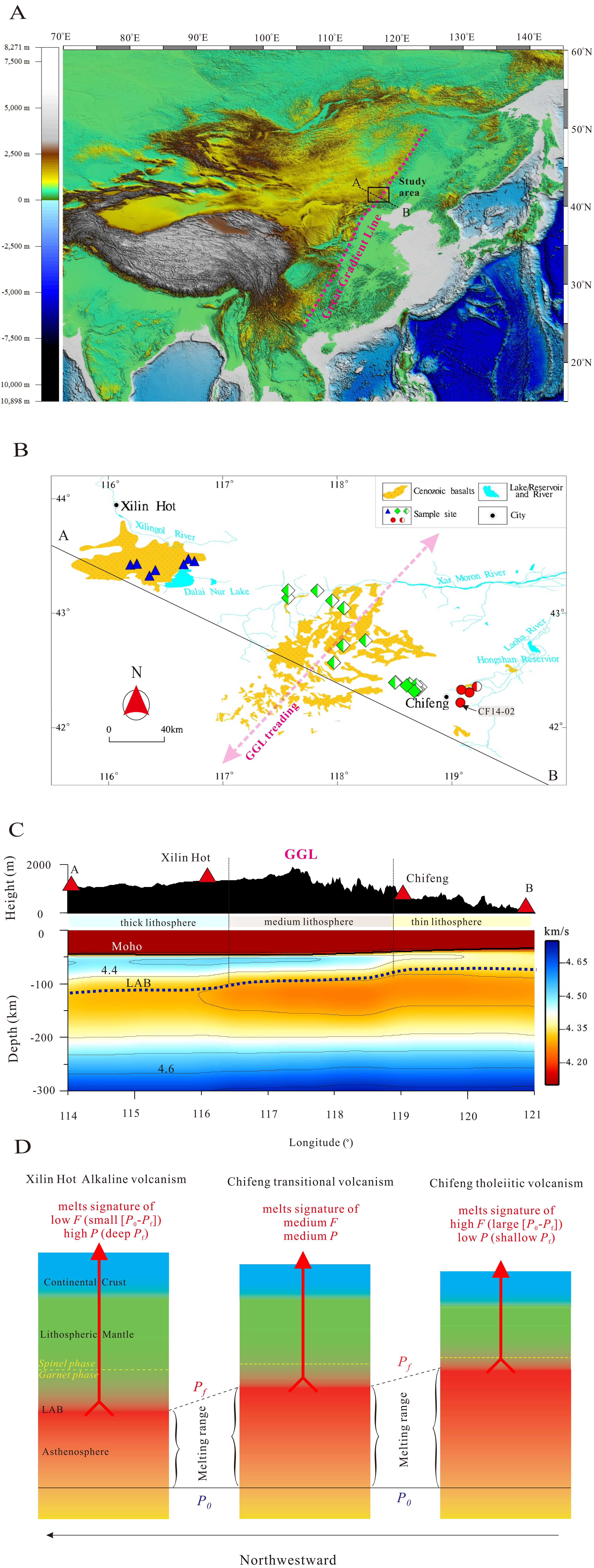

A
70°E
80°E
90°E
100°E
110°E
120°E
130°E
140°E
60°N
50°N
40°N
30°N
20°N
8,271 m
7,500 m
5,000 m
2,500 m
0 m
-2,500 m
-5,000 m
-7,500 m
-10,000 m
-10,898 m
Study area
Great Gradient Line
B
Xilin Hot
Xilingol River
Dalai Nur Lake
Xar Moron River
Lacha River
Hongshan Reservior
Chifeng
CF14-02
GGL treading
Cenozoic basalts
Lake/Reservoir and River
Sample site
City
N
0
40km
116°
117°
118°
119°
44°
43°
42°
C
Height (m)
2000
GGL
thick lithosphere
medium lithosphere
thin lithosphere
Moho
4.4
LAB
4.6
Depth (km)
-100
-200
-300
km/s
4. 65
4. 50
4. 35
4. 20
114
115
116
117
118
119
120
121
Longitude (°)
D
Xilin Hot Alkaline volcanism
melts signature of low F (small [P0-Pf]) high P (deep Pf)
Chifeng transitional volcanism
melts signature of medium F medium P
Chifeng tholeiitic volcanism
melts signature of high F (large [P0-Pf]) low P (shallow Pf)
Continental Crust
Lithospheric Mantle
Spinel phase
Garnet phase
LAB
Asthenosphere
Pf
P0
Melting range
Northwestward

Fig. 2

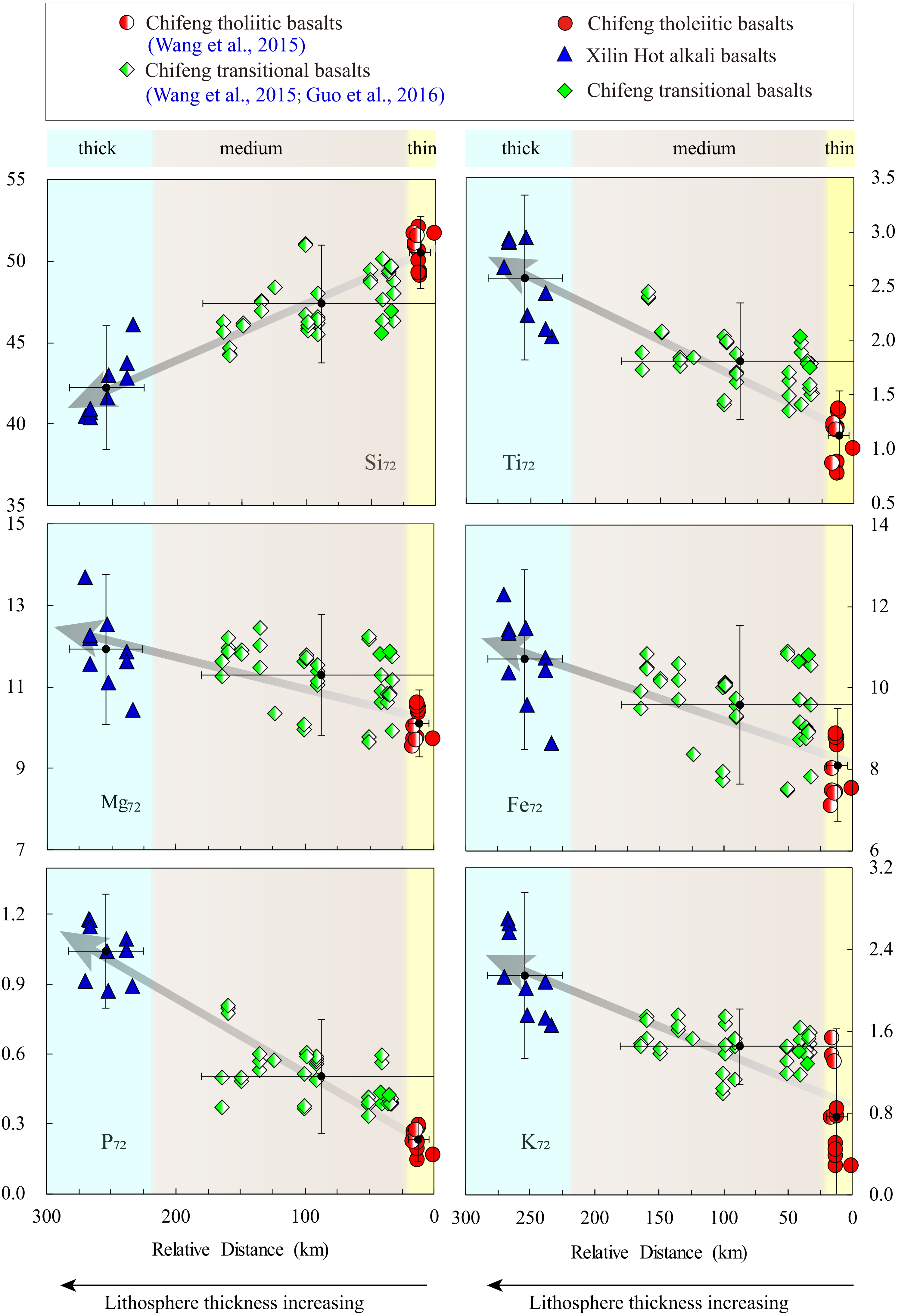

Chifeng tholiitic basalts
(Wang et al., 2015)
Chifeng transitional basalts
(Wang et al., 2015; Guo et al., 2016)
Chifeng tholeiitic basalts
Xilin Hot alkali basalts
Chifeng transitional basalts
thick
medium
thin
Si72
Ti72
Mg72
Fe72
P72
K72
Relative Distance (km)
Lithosphere thickness increasing

Fig. 3

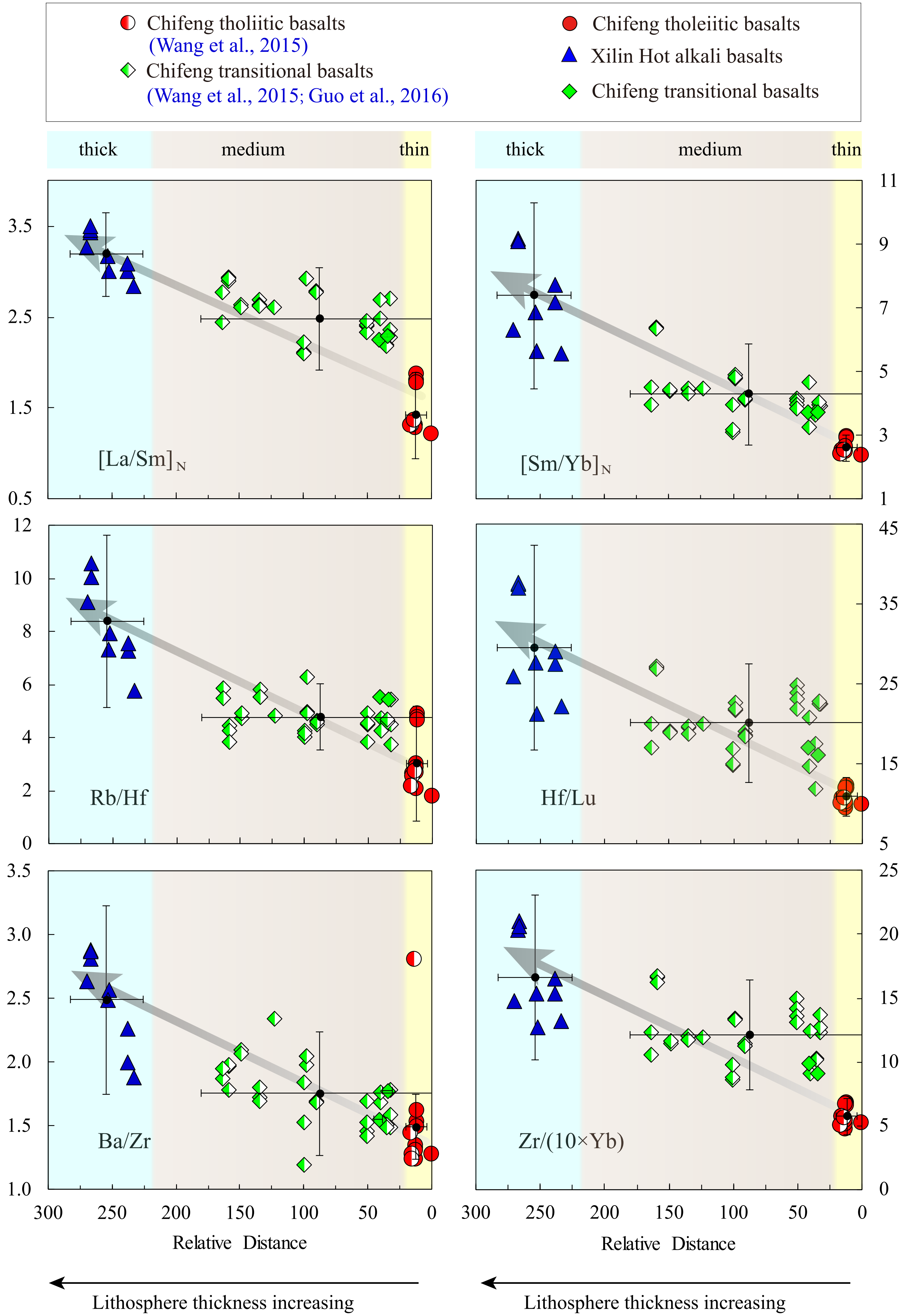

Chifeng tholiitic basalts
(Wang et al., 2015)
Chifeng transitional basalts
(Wang et al., 2015; Guo et al., 2016)
Chifeng tholeiitic basalts
Xilin Hot alkali basalts
Chifeng transitional basalts
thick
medium
thin
[La/Sm]N
[Sm/Yb]N
Rb/Hf
Hf/Lu
Ba/Zr
Zr/(10×Yb)
Relative Distance
Lithosphere thickness increasing

Fig. 4

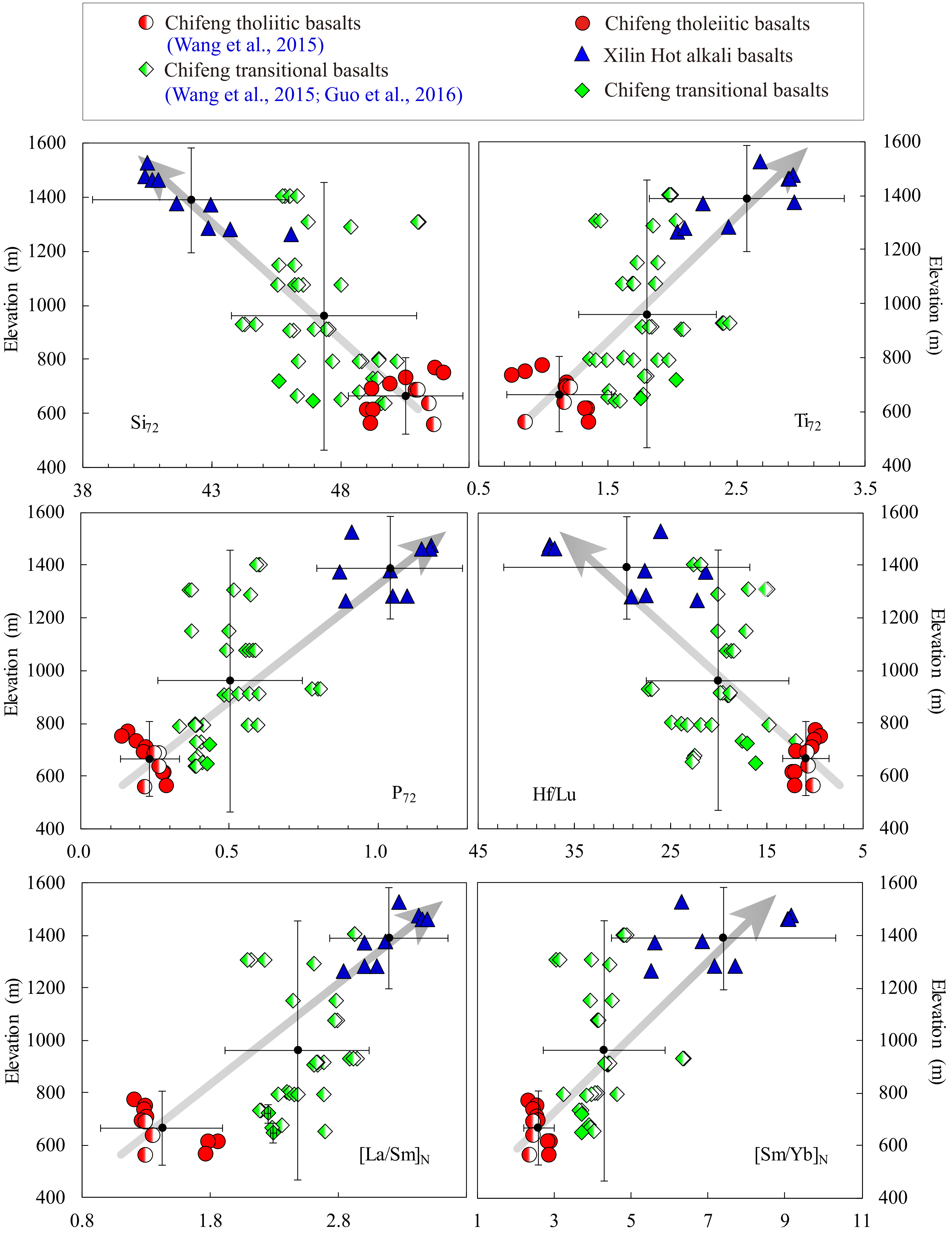

Chifeng tholiitic basalts
(Wang et al., 2015)
Chifeng transitional basalts
(Wang et al., 2015; Guo et al., 2016)
Chifeng tholeiitic basalts
Xilin Hot alkali basalts
Chifeng transitional basalts
Elevation (m)
Si72
Ti72
P72
Hf/Lu
[La/Sm]N
[Sm/Yb]N